SSRG International Journal of Electrical and Electronics Engineering
ISSN: 2348-8379/ https://doi.org/10.14445/23488379/IJEEE-V12I8P104

Volume 12 Issue 8, 29-37, August 2025

Original Article

Machine Learning-Based Severity of Critical Line for Power System Security Enhancement with Zip Loads

S. Jayakumar[1], Venkatesh Peruthambi[1*], Sudha Dukkipati[2], Pushpalatha kumari M[3], K. Manikandan[4]

[1]*Department of Electronics and Communication Engineering, Sri Sairam College of Engineering, Bengaluru, India.*
[1*]*Department of Electrical and Electronics Engineering, Mohan Babu University, Tirupati, India.*
[2]*Department of Electrical and Electronics Engineering, Koneru Lakshmaiah Education Foundation Green Fields, Vaddeswaram, Andhra Pradesh, India.*
[3]*Department of Electrical and Electronics Engineering, Ballari Institute of Technology and Management, VTU, Karnataka, India*
[4]*Department of Electrical and Electronics Engineering, Dr.Mahalingam College of Engineering and Technology, Pollachi, Tamil Nadu, India.*

[1*]*Corresponding Author : venkateshp.engg@gmail.com*

Received: 03 June 2025 Revised: 05 July 2025 Accepted: 04 August 2025 Published: 30 August 2025

Abstract *- This research proposes an advanced, data-driven framework to enhance power system security and operational reliability in the face of unforeseen faults and contingencies. A composite polynomial load model incorporating constant impedance (Z), constant current (I), and constant power (P) characteristics is employed to capture realistic load behavior under varying conditions. The methodology begins with modeling based on standard IEEE test systems, integrating this load model into power flow analysis using the Newton-Raphson algorithm. For contingency assessment, the focus is placed on single-line outage scenarios-critical events that may significantly impact system stability. A novel Hybrid Line Stability Ranking Index (HLSRI) is introduced to prioritise vulnerability, offering a more accurate ranking of transmission line criticality under stress conditions. Additionally, machine learning algorithms, including Gradient Boosting and Random Forest classifiers, are trained on system operational data to categorize the severity of line contingencies with high precision. To enhance control and stability, Flexible AC Transmission System (FACTS) devices such as the Unified Power Flow Controller (UPFC) and Interline Power Flow Controller (IPFC) are strategically deployed. Their optimal placements are determined through the metaheuristic Sparrow Search Algorithm (SSA), ensuring minimal power losses and improved dynamic performance. Simulation results validate the superiority of the proposed framework in terms of accuracy, adaptability, and system-wide resilience, making it a promising solution for real-time power grid reliability enhancement.*

Keywords *- Contingency analysis, Gradient Boosting (GB), Hybrid Line Stability Ranking Index (HLSRI), Power system security, Polynomial load model, Random Forest (RF).*

1. Introduction

The steady transformation of electrical power networks, fuelled by increasing demand, decentralized energy production, and environmental considerations, has made maintaining grid stability and security more critical than ever. Modern grids must manage a mix of renewable and conventional energy sources while dealing with sudden load variations, higher chances of faults, and more complex control challenges. As a result, system operators and planners are under constant pressure to ensure reliable operation during normal and emergency conditions. One key challenge is accurately modelling load behaviour, which plays a major role in influencing power flow, system stability, and response during faults. Although simple to compute, traditional constant load models fail to represent the true dynamic and non-linear behaviour of practical loads. The ZIP (impedance-current-power) model, commonly known as the polynomial load model, offers a more realistic load representation by combining constant impedance, current, and power characteristics. This provides a better understanding of how loads behave under varying operating conditions. Another critical aspect is pinpointing the sections of the grid that are most at risk during disturbances. Transmission line outages, especially single-line failures, can trigger chain reactions leading to voltage instability or even widespread blackouts. To address this, contingency analysis and severity ranking become essential. This study adopts a new metric called the Hybrid Line Stability Ranking Index (HLSRI) to assess the severity of line outages, offering a stronger method to identify weak links in the network [1-4].

The growth of Machine Learning (ML) in power system studies has introduced advanced methods for fault detection, classification, and prediction. In this work, Gradient Boosting and Random Forest classifiers are trained using system parameters like voltages and power flows to accurately categorize transmission lines into critical, semi-critical, and stable groups.

Since FACTS devices involve high costs and complex installations, their optimal placement is crucial. Additionally, the efficient use of generation resources with minimal fuel expenditure is equally important. For this purpose, a nature-inspired optimization technique, the Sparrow Search Algorithm (SSA), is employed to achieve optimal generation dispatch within system limits [5-9].

This paper proposes an integrated, data-driven framework combining realistic load modelling, contingency ranking with HLSRI, machine learning-based line classification, optimized FACTS deployment, and generation optimization through SSA [10-14]. The approach is validated on IEEE test systems and demonstrates excellent scalability and reliability, making it highly suitable for modern smart grid applications [15-17].

2. Problem Statement

Modern power systems have become highly intricate and often function near their stability boundaries. This heightened complexity increases the risk of disturbances, such as single-line outages, which can cause voltage instability, line overloading, and even large-scale blackouts. To maintain system reliability, stability indicators like the HLSRI are utilized. HLSRI considers factors such as power demand, transmission line impedance, and voltage levels to evaluate system margins. An HLSRI value nearing 1 indicates a heightened risk of instability. Advanced strategies, including machine learning techniques and nature-inspired optimization algorithms, are adopted to address these challenges. These methods help in the optimal placement of Flexible AC Transmission System (FACTS) devices, ensuring improved voltage regulation and enhanced system stability.

3. Methodology

The methodology starts with selecting an IEEE standard test network, such as the IEEE 30-bus system, containing detailed information on buses and transmission lines. This data is used to apply a polynomial load model based on the ZIP framework, where the load is expressed as a combination of constant impedance (Z), constant current (I), and constant power (P) elements. Active and reactive power at each bus are mathematically formulated using the following relation in eq. no 1 & 2.

$$P = P_i\left[\alpha_Z\left|\frac{V_i}{V_0}\right|^2 + \alpha_I\left|\frac{V_i}{V_0}\right| + \alpha_P\right] \tag{1}$$

$$Q = P_i\left[\alpha_Z\left|\frac{V_i}{V_0}\right|^2 + \alpha_I\left|\frac{V_i}{V_0}\right| + \alpha_P\right] \tag{2}$$

Where
P_i = Active power at bus i
Q_i = Reactive power at bus i
V_i = Voltage in p.u at bus i
V_0 = References voltage in p.u (assumed as 1.0 p.u)

$\alpha_Z, \alpha_i, \alpha_P$ There are different proportions of the total load $\alpha_Z + \alpha_i + \alpha_P = 1$.

The derived load model Equations (1) and (2) are integrated into the traditional Newton-Raphson (NR) method to analyse the load flow. After establishing the base case, different single-line outage scenarios are introduced to simulate possible faults. The HLSRI is calculated to evaluate the impact of each line outage. This index measures the combined effect of changes in bus voltages and line loading, offering a more comprehensive assessment of system vulnerability. The proposed ranking index is shown in Equation (3).

$$HLSRI = \frac{4XQ_n}{[V_m]^2}\left[\frac{|Z|^2}{X_{Line}}\beta - \frac{XQ_n}{[sin(\theta-\delta)]^2}(\beta-1)\right] \leq 1,$$
$$\text{where } \beta = \begin{Bmatrix} 1 & \delta < \delta_C \\ 0 & \delta \geq \delta_C \end{Bmatrix}, \tag{3}$$

Where δ is a modifier and β is a switching function.

The system is unstable if the HLSRI value approaches 1; otherwise, it is safe and stable. Cognitive algorithms fall into two main categories: Artificial Neural Networks (ANN) and Machine Learning (ML). For this analysis, ML is considered for further analysis. Figure 1 shows the soft-computing technique for power system security.

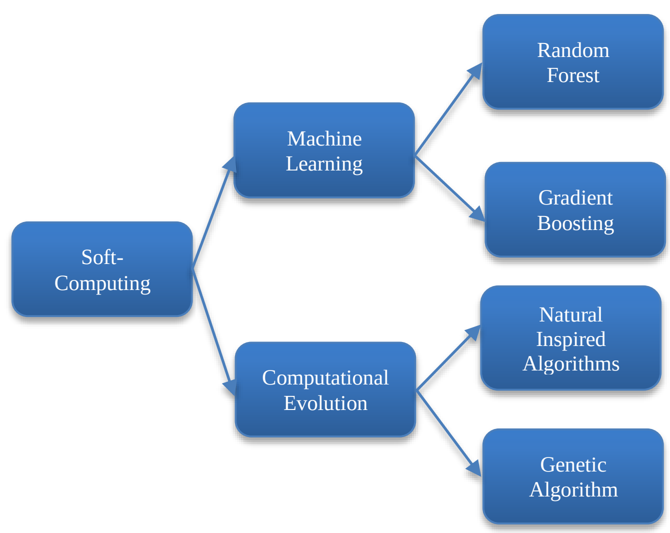

Fig. 1 Block diagram representation of soft-computing technique for power system security

4. Machine Learning Algorithm

Machine learning enables computers to learn from historical data and identify patterns without explicit programming. Instead of creating rule-based solutions, ML models learn directly from examples to perform tasks such as classification, prediction, and fault detection. A prioritized list of vulnerable transmission lines is generated using machine learning techniques. Two classifier models, namely Gradient Boosting and Random Forest, are considered. These models are trained using features like bus voltage magnitudes, phase angle differences, and corresponding HLSRI values. This approach considers six inputs (voltage, voltage angle, generation & demand of active power and HLSRI class) for training the classifier models, as shown in the equation. In the IEEE-30 bus system, 35 line outage cases were considered. Inputs to the ML model are 6. This resulted in 210 input-output data sets (35 outages * 6 states), with 175 used for training and 35 for testing the network for a clear understanding. 41 samples are considered to train the test system. Based on this training, the classifiers categorize the transmission lines into critical, semi-critical, and stable groups, aiding in better contingency planning and system strengthening. For the data analysis, 70% of the data is considered for training, and 30% of the data is considered for testing.

4.1. Random Forest (RF)

Random Forest operates by combining the outcomes of multiple simpler decision models to make more robust predictions. It showed excellent performance even when handling noisy or uncertain data, maintaining reliable classification under different operating conditions.

4.2. Gradient Boosting (GB)

Gradient Boosting is an intelligent learning model that improves step-by-step by correcting its previous errors. This study employed it to identify critical transmission lines with high precision, making it a dependable tool for assessing system risks. Gradient Boosting and Random Forest models were trained using data from various contingency scenarios.

The predictions made by these machine learning models aligned closely with expert assessments, demonstrating their reliability:

- Gradient Boosting achieved an impressive classification accuracy of 96.1%, effectively identifying the most critical transmission lines.
- Random Forest attained an accuracy of 95.3%, especially excelling when the dataset contained noise or uncertainties.

These results clearly show that machine learning techniques can play a significant role in real-time vulnerability analysis for power systems, offering fast and accurate decision support. To validate the effectiveness of these models, confusion matrices and cross-validation methods were employed. Both algorithms were trained on labeled datasets collected from different simulation cases.

Additionally, feature importance analysis was conducted to determine which electrical variables—such as voltage, power flow, and HLSRI values—had the strongest impact on predicting line vulnerability. This insight helps further refine decision-making in contingency management. The classification accuracy and misclassification rate are evaluated for the confusion matrix generated by the classifier model.

Table 1. Confession matrix for various classifier models

Classifier Type	Testing (30%)	Training (70%)
GB -classifier model	Predicted Actual $\begin{pmatrix} 2 & 0 & 0 \\ 0 & 4 & 1 \\ 0 & 0 & 6 \end{pmatrix}$	Predicted Actual $\begin{pmatrix} 3 & 0 & 0 \\ 0 & 10 & 1 \\ 0 & 2 & 12 \end{pmatrix}$
RF classifier model	Predicted Actual $\begin{pmatrix} 1 & 1 & 0 \\ 0 & 2 & 1 \\ 0 & 1 & 5 \end{pmatrix}$	Predicted Actual $\begin{pmatrix} 2 & 1 & 0 \\ 0 & 8 & 3 \\ 0 & 4 & 12 \end{pmatrix}$

From the Table 1, Classification accuracy and misclassification rate are evaluated to know the effectiveness of the classifier model.

Cassification Accurasy (CA)

$$CA(\%) = \left(\frac{No.\ of\ data\ samples\ classified\ correctly}{Total\ no.\ of data\ samples\ in\ data\ set} \right) \times 100 \tag{4}$$

Misclassification Rate (MR)

$$MR(\%) = \left(\frac{No.\ of\ misclassifications\ inclass\ Q}{Total\ no.\ of data\ samples\ in\ class\ Q} \right) \times 100 \tag{5}$$

Based on Equations (4) and (5), Table 2 is furnished and shown below.

Table 2. Classification accuracy for various classifier models

	Classifier type	CA (%)	Time (Sec)	Misclassification rate (%)		
				A	B	C
Training phase	GB	89.28	0.03	0	9.09	14.28
	RF	71.42	0.05	33.33	27.27	28.57
Testing phase	GB	92.30	0.01	0	20.00	0
	RF	84.61	0.03	50.00	20.00	16.66

Based on Table 2 above. Indicate that effective classification of critical lines is measured with high classification accuracy and a low misclassification rate. From the classifier models, the most affected line is identified from a group of critical lines, and it leads to compensation with FACTS devices (UPFC and IPFC). The mathematical model of UPFC and IPFC power injection models was deployed to improve system resilience. The voltage profile across all buses improved significantly after installation of the FACTS device.

5. Mathematical Modelling of FACTS devices

5.1. Unified Power Flow Controller (UPFC)

A powerful device that controls voltage, power flow, and stability all at once. In this project, UPFC was used to improve voltage levels and balance power flow in the grid.

$$P_{i,upfc} = [(-2R_{se} r V_i^2 \cos\gamma)/(R_{se} + X_{se})] + [(rV_i^2 X_{se} \sin\gamma)/(R_{se}^2 + X_{se}^2)] - [(R_{se} r^2 V_i^2)/(R_{se}^2 + X_{se}^2)] - [(r|V_i||V_j|X_{se} \sin(\delta_i + \gamma - \delta_j))/(R_{se}^2 + X_{se}^2)] + [(r|V_i||V_j|R_{se} \cos(\delta_i + \gamma - \delta_j))/(R_{se}^2 + X_{se}^2)] \tag{6}$$

$$Q_{i,upfc} = [(-r|V_i||V_j|)/(R_{se}^2 + X_{se}^2)] * \{X_{se} \cos\gamma - R_{se} \sin\gamma\} \tag{7}$$

$$P_{j,upfc} = [(r|V_i||V_j|)/(R_{se}^2 + X_{se}^2)] * \{R_{se} \cos(\delta_i + \gamma - \delta_j) + X_{se} \sin(\delta_i + \gamma - \delta_j)\} \tag{8}$$

$$Q_{i,upfc} = [(r|V_i||V_j|)/(R_{se}^2 + X_{se}^2)] * \{X_{se} \cos(\delta_i + \gamma - \delta_j) - R_{se} \sin(\delta_i + \gamma - \delta_j)\} \tag{9}$$

5.2. Interline Power Flow Controller (IPFC)

A smart tool that manages power across multiple transmission lines. IPFC helped reduce system losses and ensured smoother power delivery across the network.

$$P_{i,ipfc} = [(-R_{se} r V_i^2 \cos\gamma)/(R_{se} + X_{se})] + [(rV_i^2 X_{se} \sin\gamma)/(R_{se}^2 + X_{se}^2)] - [(R_{se} r^2 V_i^2)/(R_{se}^2 + X_{se}^2)] \tag{10}$$

$$Q_{i,ipfc} = [(-r|V_i||V_j|)/(R_{se}^2 + X_{se}^2)] * \{X_{se} \cos\gamma - R_{se} \sin\gamma\} \tag{11}$$

$$P_{j,ipfc} = [(r|V_i||V_j|)/(R_{se}^2 + X_{se}^2)] * \{R_{se} \cos(\delta_i + \gamma - \delta_j) + X_{se} \sin(\delta_i + \gamma - \delta_j)\} \tag{12}$$

$$Q_{i,ipfc} = [(r|V_i||V_j|)/(R_{se}^2 + X_{se}^2)] * \{X_{se} \cos(\delta_i + \gamma - \delta_j) - R_{se} \sin(\delta_i + \gamma - \delta_j)\} \tag{13}$$

Where r and γ are the control parameters of the UPFC V_i and V_j are the voltages at bus i and j; R_{se} and X_{se} are the series-connected resistance and reactance. The UPFC and IPFC models were considered with ZIP load modelling, and the performance of the test systems was investigated. Based on the literature survey, the capacity of the compensation devices is considered 30% of the line capacity and effective generation capacity allocation with SSA.

The optimization objective function minimizes real power loss and fuel cost: The objective of the rescheduling of generation is to minimize fuel cost and is defined as follows

$$Min \sum_{i \varepsilon N_g} F_T(P_{gi}) \tag{14}$$

$$F_T(P_{gi}) = a_i P_{gi}^2 + b_i P_{gi} + C_i$$

The minimization problem is subject to the following constraints

i. Power balance constraint:

$$P_{generation} = P_{Demand} + P_{Loss}$$

ii. Inequality constraints of active power generation at each unit i:

$$P_{gi}^{\min} \le P_{gi} \le P_{gi}^{\max} \qquad i = 1, \dots, N_g$$

iii. Inequality voltage constraints at each unit i:

$$V_i^{\min} \le V_i \le V_i^{\max} \qquad i = 1, \dots, N_b$$

iv. Power flow limit on transmission line:

$$S_l \le S_l^{\max}$$

The prime aim is to optimize the generation scheduling by minimizing fuel costs using nature-inspired algorithms such as Sparrow Search Algorithms (SSA). This will help to evaluate performance by rescheduling generators during contingency situations. For the purpose of maintaining the secured operating conditions for the existing demand, a reserve level was considered for the investigation. SSA: A Swarm Intelligence Optimization Algorithm for the Application to Solve Practical Engineering. SSA [11] are analysed for convergence behaviour over multiple runs and its step-by-step execution of SSA as shown in Figure 2.

These metaheuristic optimizers dynamically adjust solution paths based on fitness landscapes, ensuring that global optima for FACTS placement and sizing are reached without getting trapped in local minima.

- X-axis: Iteration count
- Y-axis: Objective function value

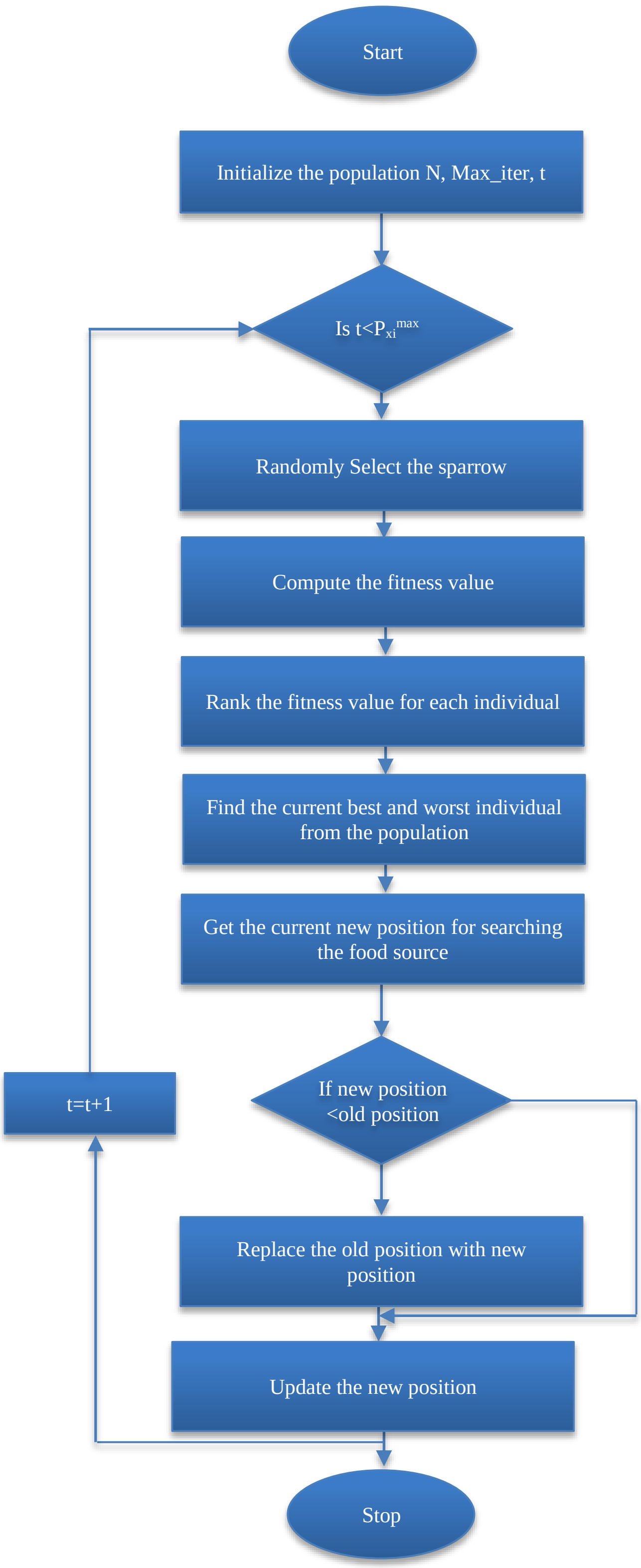

Fig. 2 Step execution of SSA flow chart

Through these analyses, the proposed framework is proven to be mathematically sound, computationally efficient, and scalable for large grid implementation.

6. Results and Discussion

To evaluate the performance of the proposed security assessment framework, extensive simulations were conducted on the IEEE 30-bus standard test systems. The study considered various loading scenarios for 24 hours, including normal base load to extreme 150% overloading conditions. This section presents a focused discussion on the results obtained from the IEEE 30-bus system using the Sparrow Search Algorithm (SSA) for effective allocation of generation capacity within the specified limits.

Table 3. Nature-inspired algorithm-based effective allocation of generation capacity with minimum fuel cost for different loads with UPFC compensation

Hour	Load Pd (MW)	Generation Pg (MW)	Power Flow (MW)	Total Losses (MW)	Fuel Cost ($/hr)
1	255.06	258.368	11.457	7.061	555.83395
2	272.064	275.876	12.305	7.550	569.92232
3	283.4	285.714	11.278	6.059	608.5838
4	297.57	300.742	17.945	6.896	608.92329
5	311.74	318.834	15.139	10.8	637.72237
6	325.91	338.372	16.205	16.067	695.72485
7	368.42	383.785	18.58	18.745	801.12955
8	396.76	416.949	19.283	23.435	869.80933
9	368.42	383.785	18.58	18.745	801.12955
10	325.91	338.372	16.205	16.067	695.72485
11	311.74	318.834	15.139	10.8	637.72237
12	297.57	300.742	17.945	6.896	608.92329
13	297.57	300.742	17.945	6.896	608.92329
14	368.42	383.785	18.58	18.745	801.12955
15	396.76	416.949	19.283	23.435	869.80933
16	410.93	430.241	20.546	22.556	883.87991
17	425.1	445.672	19.58	23.798	923.62731
18	439.27	460.934	19.625	24.823	965.76051
19	396.76	416.949	19.283	23.435	869.80933
20	340.08	354.596	19.764	18.009	704.00522
21	317.408	323.44	13.866	9.747	681.05157
22	291.902	300.714	17.359	12.509	579.83151
23	272.064	275.876	12.305	7.550	569.92232
24	255.06	258.368	11.457	7.061	555.83395

Table 4. Nature-inspired algorithm-based effective allocation of generation capacity with minimum fuel cost for different loads with IPFC compensation

Hour	Load Pd (MW)	Generation Pg (MW)	Power Flow (MW)	Total Losses (MW)	Fuel Cost ($/hr)
1	255.06	235.702	13.448	5.925	510.50
2	272.064	253.432	14.322	6.450	525.04
3	283.400	263.369	13.270	5.176	563.89
4	297.570	278.430	15.455	5.836	564.30
5	311.740	296.138	17.209	9.155	592.33
6	325.910	314.835	18.330	13.603	648.65
7	368.420	359.527	20.817	15.594	752.61

8	396.760	392.281	21.540	19.560	820.47
9	368.420	359.527	20.817	15.594	752.61
10	325.910	314.835	18.330	13.603	648.65
11	311.740	296.138	17.209	9.155	592.33
12	297.570	278.430	15.455	5.836	564.30
13	328.744	315.901	16.897	11.971	687.15
14	368.420	359.527	20.817	15.594	752.61
15	396.760	392.281	21.540	19.560	820.47
16	410.930	406.149	22.701	18.866	835.70
17	425.100	421.409	21.782	19.908	875.10
18	439.270	437.294	21.746	21.111	918.48
19	396.760	392.281	21.540	19.560	820.47
20	340.080	330.779	22.031	15.148	656.37
21	317.408	300.784	15.905	8.289	635.74
22	291.902	277.683	19.458	10.482	533.77
23	272.064	253.432	14.322	6.450	525.04
24	255.060	235.702	13.448	5.925	510.50

From Table 3 and 4, for various load demands, generation allocation using SSA with UPFC and IPFC compensation has been furnished. From the Table 5, A 24-hour dynamic simulation was conducted, and the system's response to changing demand was analyzed. From the Table 5, the minimum load and peak load are identified and summarized as follows:

- The fuel cost varied from \$510.50 during low-load hours to \$918.48 during peak demand with IPFC compensation.
- Total system losses ranged from 5.18 MW to 21.11 MW, indicating the SSA's effective control under dynamic conditions with IPFC compensation.

Table 5. Summary of minimum and peak load before and after compensation

Hour		Load (Pd)	Generation (Pg)	Power Flow (MW)	Total Losses (MW)	Fuel Cost (\$)
Min	BASE	255.06	267.923	7.92	4.95	574.94
	UPFC	255.06	258.368	11.27	6.05	555.83
	IPFC	255.06	235.70	13.45	5.18	510.50
Peak	BASE	439.27	491.829	17.96	21.18	1027.55
	UPFC	439.27	460.934	20.54	24.82	965.76
	IPFC	439.27	437.29	21.75	21.11	918.48

Figure 3 shows the demand from minimum to peak load for utilization of generation capacity with fuel cost as the base case without compensation during contingency.For more clarity of explanation, the total power transfer capability and losses shown in Figure 4, and the total generation capacity with minimum fuel cost with compensation (UPFC) are shown in Figure 5 as follows:

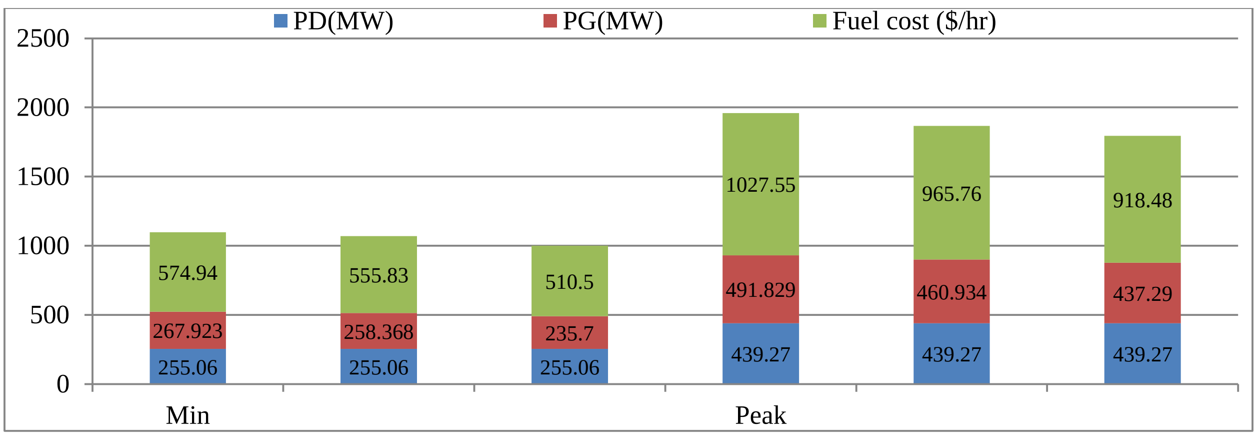

Fig. 3 Total generation capacity, demand and fuel cost for min and peak load model

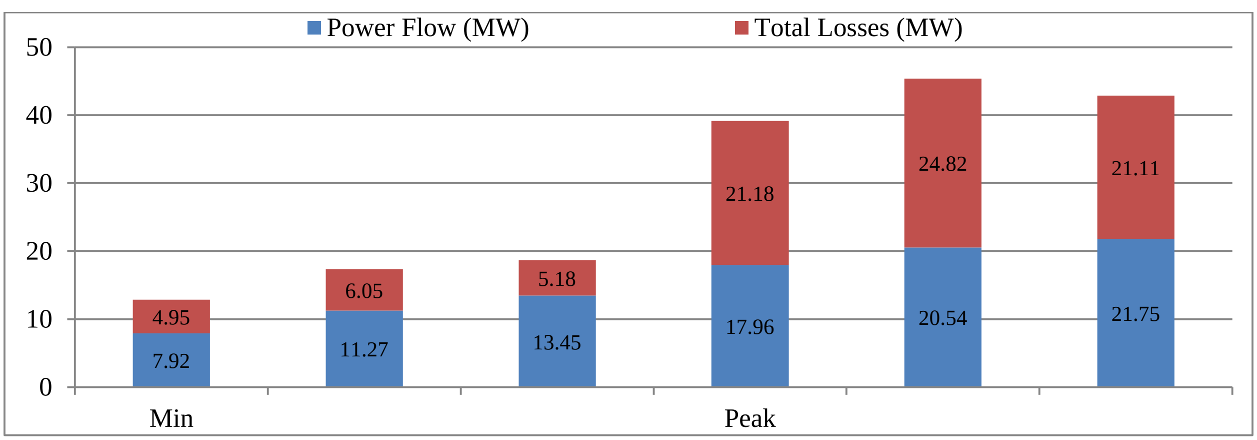

Fig. 4 power transfer capability and total system losses for the min and peak load model with compensation

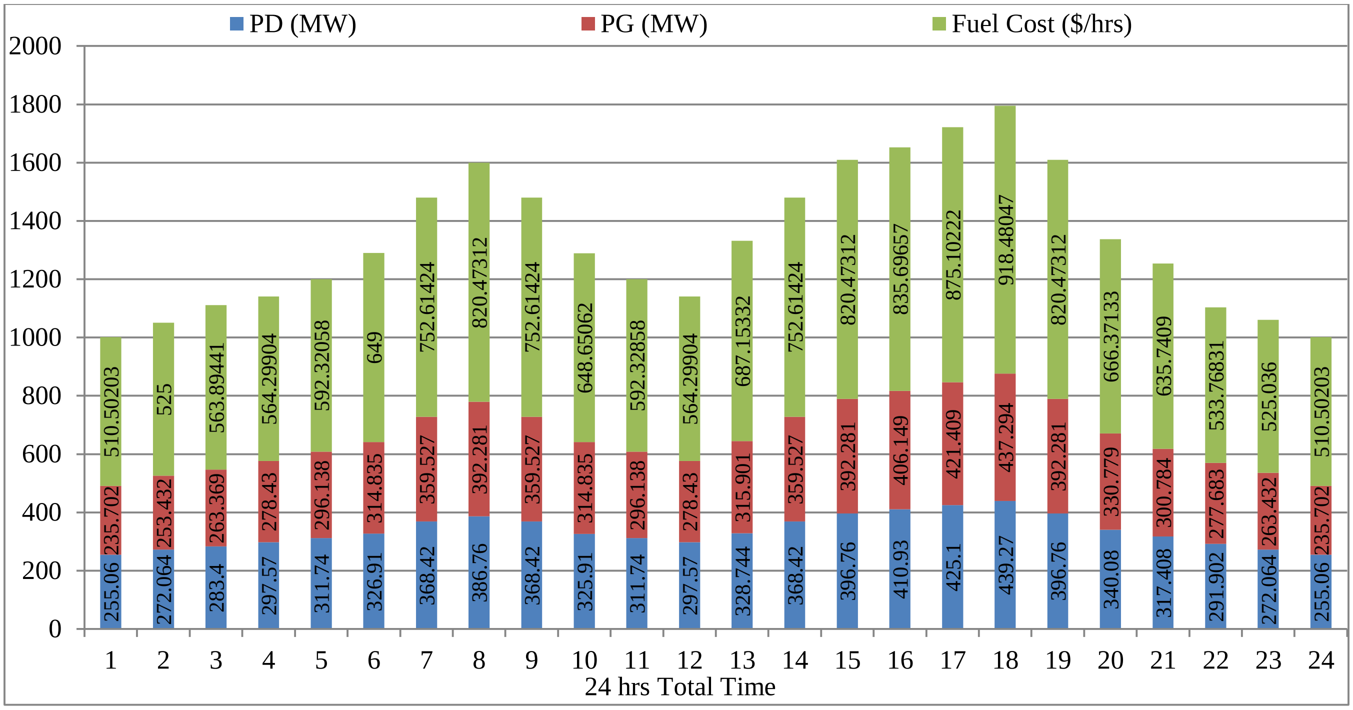

Fig. 5 SSA-based total generation capacity with minimum fuel cost based on the 24-hour demand with UPFC compensation

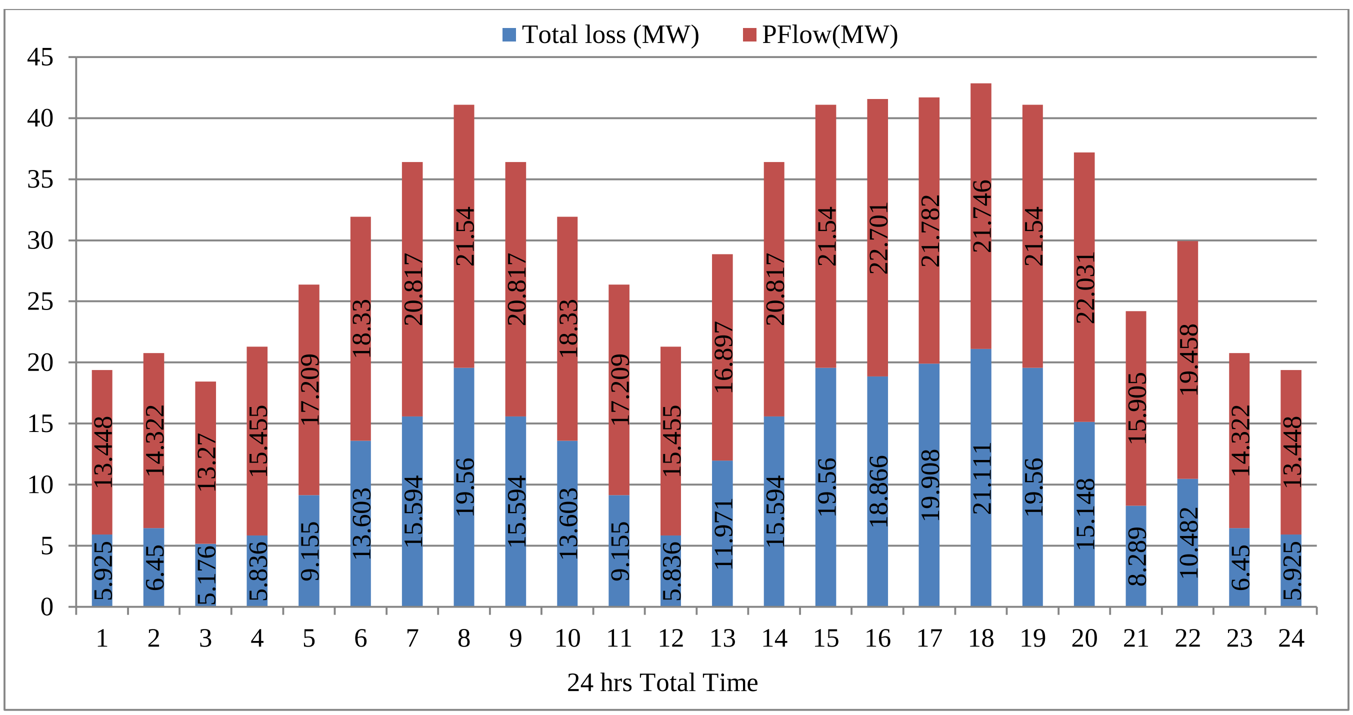

Fig. 6 Power flows and total system losses for the 24-hour demand with UPFC compensation

Figures 3 and 4 show the total generation capacity with minimum fuel cost during minimum and peak load demand. Figure 5 shows the SSA-based total generation capacity with minimum fuel cost based on the 24-hour demand with UPFC compensation. Similarly, IPFC compensation along with SSA is used, as shown in Figures 7 and 8. From Figures 5 to 8, it is clear that the total system losses are reduced by effective allocation of generation capacity with and without compensation by identifying the most affected line using Machine learning classifier models and algorithms.

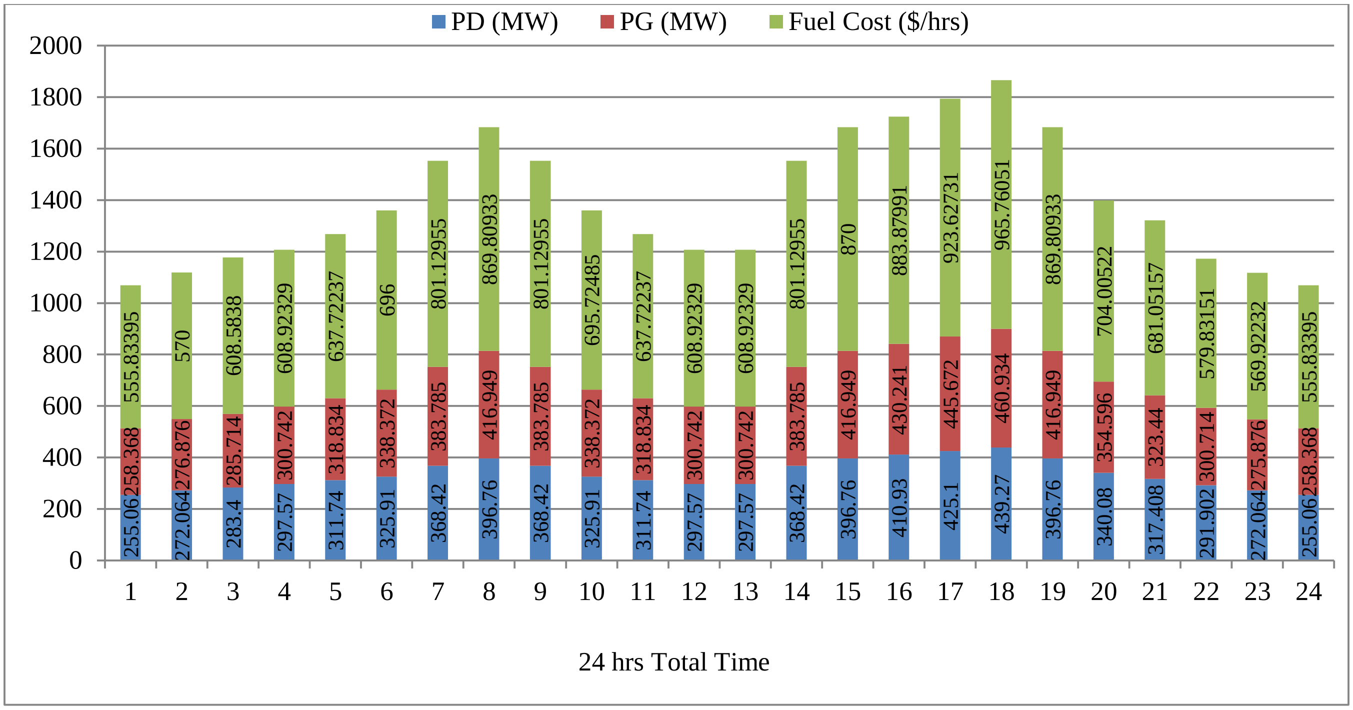

Fig. 7 SSA-based total generation capacity with minimum fuel cost based on the 24-hour demand with IPFC compensation

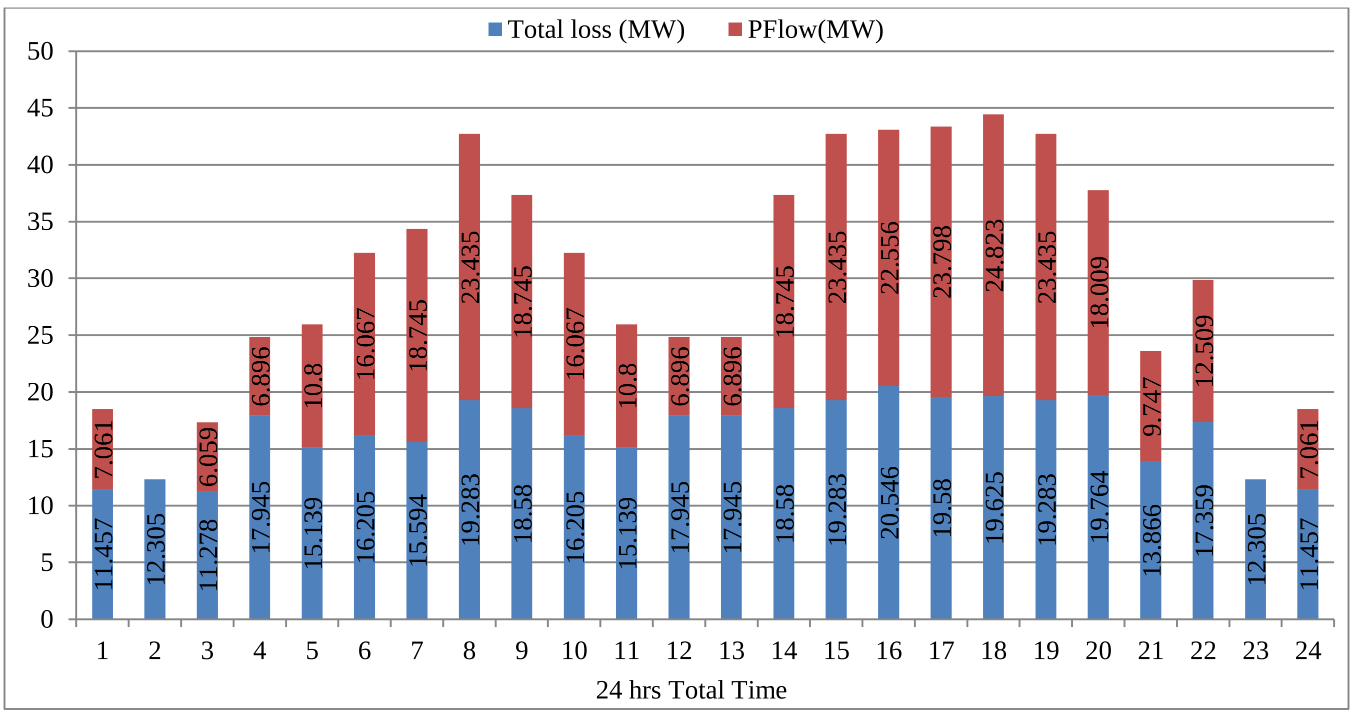

Fig. 8 Power flows and total system losses for the 24-hour demand with UPFC compensation

7. Conclusions

This research presents a comprehensive, intelligent framework for securing power systems under contingency scenarios. By integrating ZIP-based load modeling with Newton-Raphson load flow, the system gains an accurate and reliable starting point for analyzing power distribution.

The introduction of the HLSRI offers a robust method for identifying and quantifying the severity of single-line outages. Unlike conventional methods, this approach enhances outage ranking accuracy and provides a deeper understanding of system vulnerabilities.

The use of modern machine learning techniques such as Random Forest and Gradient Boosting further streamlines the classification of critical lines, offering high accuracy and fast decision-making capabilities. The proposed system was tested under varying load conditions using IEEE standard test cases and consistently demonstrated excellent performance. The approach is adaptable, scalable, and can be extended to more complex, real-time grid scenarios.

References

[1] Reynato Andal Gamboa, Chockalingam Aravind Vaithilingam, and Chew Ai Chin, "Power System Network Contingency Studies," *2018 IEEE Student Conference on Research and Development (SCOReD)*, Selangor, Malaysia, pp. 1-6, 2018. [CrossRef] [Google Scholar] [Publisher Link]

[2] Jothy Venkateswaran et al., "Contingency Analysis of an IEEE 30 Bus System," *2018 3rd IEEE International Conference on Recent Trends in Electronics, Information & Communication Technology (RTEICT)*, Bangalore, India, pp. 328-333, 2018. [CrossRef] [Google Scholar] [Publisher Link]

[3] Anmar Arif et al., "Load Modeling - A Review," *IEEE Transactions on Smart Grid*, vol. 9, no. 6, pp. 5986-5999, 2018. [CrossRef] [Google Scholar] [Publisher Link]

[4] Partha P. Biswas et al., "Optimal Placement and Sizing of FACTS Devices for Optimal Power Flow in a Wind Power Integrated Electrical Network," *Neural Computing and Applications*, vol. 33, no. 12, pp. 6753-6774, 2021. [CrossRef] [Google Scholar] [Publisher Link]

[5] Ahmed Nasser Alsammak, and Hasan Adnan Mohammed, "A Literature Review on the Unified Power Flow Controller UPFC," *International Journal of Computer Applications*, vol. 182, no. 12. pp. 23-29, 2018. [CrossRef] [Google Scholar] [Publisher Link]

[6] Parimal Acharjee, "Optimal Power Flow with UPFC using Security Constrained Self-Adaptive Differential Evolutionary Algorithm for Restructured Power System," *International Journal of Electrical Power & Energy Systems*, vol. 76, pp. 69-81, 2016. [CrossRef] [Google Scholar] [Publisher Link]

[7] Sankalp Asawa, and Sam Al-Attiyah, "Impact of FACTS Device in Electrical Power System," *2016 International Conference on Electrical, Electronics, and Optimization Techniques (ICEEOT)*, Chennai, India, pp. 2488-2495, 2016. [CrossRef] [Google Scholar] [Publisher Link]

[8] Ayman Alhejji et al., "Optimal Power Flow Solution with an Embedded Center-Node Unified Power Flow Controller Using an Adaptive Grasshopper Optimization Algorithm," *IEEE Access*, vol. 8, pp. 119020-119037, 2020. [CrossRef] [Google Scholar] [Publisher Link]

[9] Sai Ram Seshapalli, "Analysis of Hybrid Power Flow Controller using Static Load Model under Contingency Screening," *2019 IEEE International Conference on Clean Energy and Energy Efficient Electronics Circuit for Sustainable Development (INCCES)*, Krishnankoil, India, pp. 1-6, 2019. [CrossRef] [Google Scholar] [Publisher Link]

[10] Akanksha Mishra, and G.V. Nagesh Kumar, "A Risk of Severity Based Scheme for Optimal Placement of Interline Power Flow Controller Using Composite Index," *International Journal of Power and Energy Conversion*, vol. 8, no. 3, pp. 257-275, 2017. [CrossRef] [Google Scholar] [Publisher Link]

[11] Siavash Yari, and Hamid Khoshkhoo, "Assessment of Line Stability Indices in Detection of Voltage Stability Status," *2017 IEEE International Conference on Environment and Electrical Engineering and 2017 IEEE Industrial and Commercial Power Systems Europe (EEEIC / I&CPS Europe)*, Milan, Italy, pp. 1-5, 2017. [CrossRef] [Google Scholar] [Publisher Link]

[12] Abdelfattah A. Eladl, Mohamed I. Basha, and Azza A. ElDesouky, "Multi-Objective-Based Reactive Power Planning and Voltage Stability Enhancement Using FACTS and Capacitor Banks," *Electrical Engineering*, vol. 104, no. 5, pp. 3173-3196, 2022. [CrossRef] [Google Scholar] [Publisher Link]

[13] Aditya Chorghade, and Vandana A. Kulkarni Deodhar, "FACTS Devices for Reactive Power Compensation and Power Flow Control - Recent Trends," *2020 International Conference on Industry 4.0 Technology (I4Tech)*, Pune, India, pp. 217-221, 2020. [CrossRef] [Google Scholar] [Publisher Link]

[14] N.S. Goutham, and Mohd. Z.A. Ansari, "Determination of Optimal Location of FACTS Devices for Power System Restoration Including Load Flow and Contingency Analysis," *International Journal of Engineering Research and Technology (IJERT)*, vol. 5, no. 18, pp. 1-4, 2017. [Google Scholar] [Publisher Link]

[15] Krishnan Suresh, and Ezhilvannan Parimalasundar, "Design and Implementation of Universal Converter Design and Implementation of a Universal Converter," *IEEE Canadian Journal of Electrical and Computer Engineering*, vol. 45, no. 3, pp. 272-278, 2022. [CrossRef] [Google Scholar] [Publisher Link]

[16] Parimalasundar Ezhilvannan, and Suresh Krishnan, "An Efficient Asymmetric Direct Current (DC) Source Configured Switched Capacitor Multi-Level Inverter," *European Journal of Automated Systems*, vol. 53, no. 6, pp. 853-859, 2020. [CrossRef] [Google Scholar] [Publisher Link]

[17] Biplab Bhattacharyya, and Saurav Raj, "Swarm Intelligence Based Algorithms for Reactive Power Planning with Flexible AC Transmission System Devices," *International Journal of Electrical Power & Energy Systems*, vol. 78, pp. 158-164, 2016. [CrossRef] [Google Scholar] [Publisher Link]